Statistical Characteristics of Aircraft Arrival Tracks

John F. Shortle*
Systems Engineering and Operations Research
Center for Air Transportation Systems Research
George Mason University
4400 University Dr., MS 4A6
Fairfax, VA 22030
Tel: 703-993-3571
Fax: 703-993-1521
e-mail: jshortle@gmu.edu

Yimin Zhang
George Mason University
4400 University Dr., MS 4A6
Fairfax, VA 22030
Fax: 703-993-1521
e-mail: yzhangk@gmu.edu

Juan Wang
George Mason University
4400 University Dr., MS 4A6
Fairfax, VA 22030
Fax: 703-993-1521
e-mail: jwangl@gmu.edu

* Corresponding author

Word Count: 4,708
Number of Figures: 9
Submission Date: 3/15/10

ABSTRACT

The statistical characterization of flight tracks is a critical component of safety-analysis models. This paper presents an analysis of multilateration data using an extension of an algorithm given in Jeddi et al. (2006). Key results are as follows. The separation distribution does not appear to change much at different points along the approach path. The left tail of separation (corresponding to the smallest separation values) does not appear to be heavy-tailed. This is positive from a safety perspective. If we extrapolate this behavior beyond the observed data, we conjecture that smaller separations have probabilities that rapidly decay to effectively zero. Lateral positions near the threshold do not appear to be heavy tailed either. Finally, estimates of the final-approach separation variability are consistent with previously published results.

INTRODUCTION

The objective of this paper is to characterize statistical properties of aircraft flight tracks of arrivals to a major U.S. airport. A statistical characterization of flight tracks is useful for a variety of reasons.

First, the statistical distributions are critical in many quantitative safety analyses. For example, in the analysis of wake vortex encounters (e.g., *1*,*2*), the distribution of airplane locations is important for determining the fraction of flights that may encounter a wake. Of particular importance is the *tail behavior* – that is, the extremely large values and/or the extremely small values of the distribution. For example, wake encounters are more likely to occur when the separation time is unusually small and/or when the trailing aircraft is at an unusually low altitude and/or when the leading aircraft is at an unusually high altitude (this is because wakes tend to sink). If the extreme values of the distribution can be reduced, then the safety of the system may improve.

A second benefit is to identify potential benefits of new concepts and technologies that reduce the variance in aircraft positions. For example, required navigation performance (RNP) reduces the region of space in which an aircraft is likely to be found. Trajectory-based operations reduce the variability of separation in time by providing time requirements for passing certain waypoints. A reduction in separation variance provides an indirect improvement in capacity. Because the extremely short separation times are eliminated, the target separation can be reduced, thus improving capacity, while maintaining or improving the existing level of safety.

Several researchers have measured the statistical distributions of aircraft separations on arrival, both in terms of distance and time. References (*3*, *4*, *5*) measured the separation times by direct observation of airport operations. Others have obtained similar distributions using radar data (*6*, *7*, *8*) and multilateration data (*9*, *10*, *11*). Reference (*12*) uses multilateration data to obtain estimates of lateral position on approach. This paper extends and revises the algorithms given in (*10*). A key contribution of this paper is to obtain results related to the extreme values of the distributions using a larger number of tracks (nearly a year of data). For aircraft-position deviations in the en-route environment, see for example (*13*, *14*, *15*).

METHODOLOGY

Multilateration systems collect aircraft position data by computing the time difference of transponder signals to multiple receiving stations. The update rate is about once per second, faster than the update rates of standard radar (once every 4+ seconds). This paper utilizes multilateration data collected at Detroit Metropolitan Wayne County airport (DTW) during 2003.

We describe an algorithm for processing multilateration data based on an algorithm given in (*10*). Step 6 and most of step 8 are new. The other steps have been modified slightly from the original. We include the entire description for completeness. The algorithm is now in C++ instead of MATLAB which significantly increases its speed. Previously, it took approximately one week of computer time to process one month of data for one runway. Now it takes about 2 hours. This allows for a larger volume of data to be processed – almost one year of data here versus one week of data in (*10*).

Step 1: Convert data to text file. The input data consist of a single table with five fields: Aircraft mode-S, time, *x*-coordinate, *y*-coordinate, and mode-C. The mode-S value uniquely identifies a physical aircraft. The mode-C value is a barometer-based measurement that can be used to estimate altitude in meters = (25 x Mode-C – 10,000) x .3048, where .3048 converts feet to meters.

Step 2: Rotation. The coordinates of the original data are aligned with true north and true east. The origin is located at the control tower (Figure 1). We first rotate the coordinate system so that the *x*-axis is aligned with the runway in question. Then, we translate the coordinate system so that the origin is located at the threshold of the runway (as in Figure 2); see also (*10*) for further details.

Step 3: Boxing. We create two boxes near the runway of interest with dimensions as shown in Figure 2. All points that are outside of the two boxes are discarded. Figure 2 shows the results of this step applied to a single day of data. In this step, we also convert the mode-C value to altitude for each point.

Step 4: Extract individual tracks. Roughly speaking, we define a "track" to be a set of points corresponding to one operation (an arrival or departure or possibly a go-around or flyover). At this point, the data consist of a long list of multilateration points, but there is no designation that any particular set of points should be grouped together to form a single operation. The objective of this step is to take the long list and identify break points where one track ends and another begins.

We first sort the boxed data (from Step 3) by mode-S and then by time. In this way, all points associated with a given physical aircraft are located together in the data set. A record is assumed to be the start of a new track if any of the three conditions holds:

1) Its mode-S value is different than the mode-S of the previous record, or
2) There is a time gap of more than 60 seconds from the previous record, or
3) There is a change in (non-vertical) distance greater than 0.4 nm from the previous record.

The last two steps assume that if there is a gap in time or distance between two successive measured positions of the same aircraft, then the two positions correspond to different operations. For example, this could correspond to an aircraft that departs the airspace then arrives a significant time later. These conditions can also be triggered by missing data. In such a case, one arrival may be split into two separate "tracks". In subsequent steps, these two "half-tracks" will be discarded due to data-integrity checks described later. The end effect is that these conditions ensure that no tracks have any gaps in time greater than 60 seconds or gaps in distance greater than 0.4 nm.

Step 5: Identify arrival tracks. A track is considered an arrival if all of the following are true:

1) The first point of the track is at least 2 nm prior to the threshold (Figure 2),
2) The last point of the track is at least 0.15 nm beyond the threshold,
3) When the aircraft crosses the threshold of the runway, its lateral position is within the width of the runway.

The first two conditions identify arrivals versus departures and also ensure that the track has sufficient data and does not have gaps. The last condition helps to eliminate flyovers that otherwise satisfy the first two conditions.

Step 6: Adjust altitude measurements. The altitude measurements come from mode-C pressure measurements, rather than from multilateration data. Figure 3 shows the track of one sample landing. The black lines denote the original measurements. There are a number of missing or "zero" values. Also, some values appear to abruptly "pop up" or "pop down" from the true trajectory. It is non-trivial to determine which values are "bad" and which values are correct. We describe a heuristic which attempts to identify and correct the bad altitude measurements. The heuristic is not *guaranteed* to produce more accurate results but rather is based on a set of rules that *appear* to give improved results. Figure 3 shows the original and adjusted values. (The step-like behavior of the data is due to the discrete nature of the mode-C reading.)

The heuristic for adjusting the altitude measurements is as follows:

1. All altitude measurements are renormalized so that the runway is at height 0. Specifically, the measured altitude when the airplane is on the runway is subtracted from every altitude measurement.
2. To adjust the altitude measurements, two steps are made in order:
    a. For each point, if the altitude is more than 150 feet away from the average of the two adjacent points, then the point is discarded.
    b. For each point, if the slope of the point compared with the last valid point is greater than 0.2, then the point is discarded. (The idea is that abrupt changes in altitude are an indication of bad data).
3. The eliminated altitude values are replaced using linear interpolation using the nearest points with valid altitude values.

Some tracks are missing *all* altitude measurements. In this case, the track is kept without any altitude information, since the lateral and longitudinal positions still provide useful information for aircraft separation.

Step 7: Collect track statistics at a given longitudinal position. Each track represents a path in three dimensions $\{x(t), y(t), z(t)\}$. This step extracts the lateral and vertical position of the aircraft (y and z) as it crosses a given longitudinal position x. (This is done via interpolation when the individual track points do not lie exactly at the specified longitudinal position). The result is a "snapshot" of the aircraft positions at certain distances from the threshold. Finally, we determine the time separation (at a given longitudinal position) by sorting the points according to time and computing the difference in time between two successive aircraft as they pass through the specified longitudinal position.

Step 8: Collect other track information. In this step, we collect other pieces of information associated with each track. These include:

- IMC/VMC. We determine whether or not an arrival was flown under IMC or VMC conditions using the IMC/VMC flag in the ASPM database. The ASPM data is linked to the multilateration data using the time

and date fields (and by appropriately converting GMT to local time). Specifically, the time of the earliest data point in a given multilateration track is used as the linking key for the ASPM database.

- Wind speed and direction. This is obtained from the ASPM database in a similar manner.
- Average ground speed. Ground speed is computed as the distance between two multilateration records divided by the time difference between the records. Because of challenges in computing a derivative over small time scales, we use an average here. One point used in the speed calculation is the earliest point of the track that is within 100 ft of the centerline of the runway. The other point is the point where the aircraft crosses the threshold. The ground speed is the Euclidean distance between these points divided by the difference in time.
- Average air speed. Air speed is computed by appropriately combining the ground speed and the component of wind speed aligned in the direction of the runway.

As a validation check, Figure 4 shows a comparison of the arrival counts observed in the ASPM database and the arrival counts observed from the multilateration data (a similar check was conducted in (*10*)). There are two key observations from the figure. First, the multilateration counts are less than the ASPM counts. This is expected. We deliberately designed the multilateration processing algorithms to remove tracks that fail any of a number of data integrity checks (e.g., missing data, noisy data, etc.). Thus, we expect to remove a certain number of multilateration tracks in order to ensure that the remaining tracks pass a data quality threshold. Second, there is still agreement between the *timing* of the two data series (that is, where the peaks and valleys lie). The main purpose of this exercise is to validate that the linking of the two datasets via the date/time field is correct. Thus, we can be confident that each multilateration track is appropriately matched with the fields pulled from the ASPM database (e.g., IMC/VMC).

RESULTS

Regarding the accuracy of the multilateration system, it is difficult to specify precisely. But inspection of the data can reveal some approximate values. The observed standard deviation of lateral position at the threshold is about 10 feet. Thus, two or three standard deviations give a rough order-of-magnitude upper bound on the measurement errors *at the threshold*. However, the multilateration accuracy may degrade at larger distances from the threshold, so the results in this section focus on data at or near the threshold.

Results in this section are based on arrivals to runways 22R and 21L. On runway 22R, about 38,700 valid tracks were obtained from 10 months of data (Jan. – Oct. 2003; about 7,700 tracks during IMC and about 31,000 tracks during VMC). On runway 21L, about 8,000 tracks were obtained from 2 months of data (Jan. – Feb. 2003; about 2,500 tracks during IMC and about 5,500 tracks during VMC). Many tracks are thrown away due to data integrity issues, so these numbers represent lower bounds on the actual number of arrivals. Unless specified otherwise, all figures in this section represent data during both IMC and VMC.

Figure 5 shows the separation distribution at the threshold of runway 22R, broken down by VMC and IMC. As expected, the VMC separations are smaller on average than the IMC separations. The VMC curve is smoother than the IMC curve because it is based on a larger sample size. IMC and VMC are defined by weather minima at the airport. In this paper, the conditions are determined by looking up the IMC/VMC flag in the ASPM database. Small separations in IMC are not necessarily violations, because pilots may accept responsibility for separation provided the leading aircraft can be seen (*16*, section 7-4-3). Also, separation standards are given in terms of *distance*, while the data here are given in terms of *time*. (The two can be approximately related given the aircraft velocity. As an example, assuming a constant final approach speed of 140 knots, a time separation of 60 seconds corresponds to a distance separation of about 2.3 nm.)

Variability in the separation distribution can be seen as coming from two sources. The first source is the timing of aircraft arriving to the terminal area. During low demand periods, there may be large gaps in the arrival process. This variability is associated with the right side of the separation distribution. This variability is "external" in the sense that low demand periods are often determined by the schedule rather than by noise in the system. The second source of variability arises from control of aircraft within the terminal area to the threshold. Ideally, during periods of high demand, aircraft arrive at the threshold at precisely spaced time intervals. However, due to uncertainties in wind, aircraft speed, and so forth, there is some variability about the target separation. This "final approach variability" is associated with the *left* side of the distribution.

Typically, this variability is modeled as a normal distribution (e.g., *17*). Reference (*3*) uses a gamma distribution. Estimates for the standard deviation typically fall in the range of 15-20 seconds – for example, 18 seconds (*18*), 17.7 seconds (*7*), 19-20 seconds (*6*), and 14.5-21 seconds (*3*). We estimate this variability by fitting a

normal distribution (specifically, the left half of a normal distribution) to the portion of the separation distribution lying to the left of the mode. The corresponding standard deviation for IMC tracks for arrivals to 21L is about 17.5 seconds, which is consistent with previous results. (The studies listed here consider different airports and weather conditions, so the results are not perfectly comparable against each other.)

Because of variability in separation times, a buffer is typically added to the minimum separation (e.g., *19*). One commonly used modeling framework is given in (*17*). In this framework the separation time equals a separation standard plus a buffer plus the final approach variability plus the demand variability. In practice, the applied buffer has been observed to be approximately one standard deviation of the final approach variability (*3*, p. 44). Technologies that reduce this variability have the potential to increase capacity. This is because a smaller variability on the left side of the distribution means that a smaller buffer is needed, which allows for tighter spacing of aircraft. The corresponding relationship between capacity and variance has been analyzed in (*19*).

Figure 6 shows how the separation distribution varies in terms of distance to the threshold. The dot is the median observation. The box specifies the 25% quantile and the 75% quantile. The size of the box is defined as the inter-quartile range. As airplanes get closer to the runway, there is a slight increase in the size of the inter-quartile range, denoting a slight increase in separation variability. However, the median separations and lower 25% quantiles are relatively constant indicating that the left tails of the distribution are very similar as a function of distance to the threshold. (The upper adjacent value is the largest observation that is less than or equal to the upper quartile plus 1.5*r*, where *r* is the inter-quartile range. The lower adjacent value is the smallest observation that is greater than or equal to the lower quartile minus 1.5*r*. The outliers, beyond the adjacent values, give the extreme value of the distribution.)

The left side of Figure 7 shows a top-level view of one day of flight tracks arriving to runway 21L. The points are color-coded based on weather conditions (IMC or VMC). In IMC, aircraft fly through the final approach fix straight to the runway. In VMC, it is possible for aircraft to intercept the approach course after the final approach fix. The tracks in the figure are consistent with these rules. The right figure shows the sample PDF of the lateral position (based on 2 months of data for runway 21L) at a point 4 nm from the runway. Note that there may be some inaccuracies in the data at this distance from the threshold. Nevertheless, as expected from a qualitative perspective, the right tail of the distribution is "heavier" in VMC than in IMC. This corresponds to tracks that curve in from the side.

We now investigate the tail behavior of the distributions. From a safety perspective, the tail behavior governs the frequency with which extremely large or extremely small values are observed. Different kinds of distributions yield vastly different extreme-event probabilities, so it is important to classify the tail behavior well. The previous figures focused more on the *bodies* of the distributions. Now we take a closer look at the tails.

A commonly used distribution is the normal distribution. From a rare-events perspective, the normal distribution is said to be *light-tailed*. Intuitively, this means that the probability of observing a large event is extremely small. The probability drops off very rapidly as the value in question gets larger and larger. At some point, the probability of an extreme event is effectively zero. In contrast, a *heavy-tailed* distribution has a non-trivial probability of yielding an extremely large value. Examples are distributions that decay according to a power law, such as the distribution of file sizes on the Internet or the distribution of insurance claim sizes. A critical question from a safety perspective is: Do extreme events occur with effectively zero probability, as in the light-tailed case, or do they occur with some small but non-trivial probability, as in the heavy-tailed case?

The tail behavior of a distribution is described by its cumulative distribution function (CDF) $F(x)$ or by its complementary CDF (CCDF) $F^c(x) = 1 - F(x)$. Some common distributions and their associated tail-decay rates are:

- Standard-normal-distribution decay: $F^c(x) \sim c\, x^{-1} \exp(-ax^2)$,
- Exponential decay: $F^c(x) \sim c \exp(-ax)$,
- Power-law decay: $F^c(x) \sim c\, x^{-a}$,

where a and c are constants, and $f(x) \sim g(x)$ if $f(x) / g(x)$ goes to 1 as x goes to infinity. Of these distributions, the normal distribution has the lightest tail, and the power law has the heaviest tail.

We can roughly determine the rate of decay by plotting the sample CDF or CCDF of the distribution and noting the shape. In particular, certain transformations of each distribution lead to a linear relationship. Creating the desired plot and checking for linearity in the extreme values gives a rough way to characterize the tail behavior. For example, the CCDF of an exponential distribution is $F^c(x) \sim \exp(-ax)$. Taking the natural log of both sides gives $\ln[F^c(x)] \sim -ax$. So, a plot of $\ln[F^c(x)]$ versus x yields a straight line. Similarly, a plot of $\ln[-\ln[F^c(x)]]$ versus $\ln[x]$ gives a straight line of slope b if $F^c(x) \sim c \exp(-ax^b)$, where $b = 1$ corresponds to exponential decay, $b = 2$ is similar to normal decay, and larger values of b correspond to faster decay.

We show a few representative results. Figure 8 shows a plot related to the left tail of separation time based on ten months of data for runway 22R (approximately 38,700 tracks in both IMC and VMC). The values on the *right*

side of the graph correspond to the *smallest* observed separation times. The slope of the graph gives an estimate of the tail parameter *b*. For separation times around 75 seconds, the slope is around 1.0, corresponding to exponential decay. For smaller separation times, the slope increases to 2.0, corresponding to normal-like decay. For the extreme values of the tail (below 50 seconds), the slope is above 2.0, corresponding to faster-than-normal decay. (To construct the figure, the data are first centered about the mode of the distribution which is approximately 100 seconds.)

Figure 9 shows the tail behavior of lateral position for runway 21L, 1 nm from the threshold. The left and right tails of lateral position follow exponential decay. This is shown by the linear behavior in both graphs of $\ln[F(y)]$ and $\ln[F^c(y)]$ versus $\ln[y]$. The figure does not imply that the entire distribution of lateral position is an exponential distribution, but rather that the left and right tails follow exponential decay.

Neither separation times nor lateral positions appear to have a power tail. This is positive from a safety perspective, because it means that larger lateral deviations and shorter separation times are extremely rare and can rapidly approach a point where the probability is effectively zero. This asymptotic tail behavior is also consistent with results for altitude deviations en-route (*14*) in which the tail-decay rate is estimated to be between exponential and normal.

CONCLUSIONS

The statistical characterization of flight tracks is a critical component of safety-analysis models. This paper presented an analysis of multilateration data using an extension of an algorithm given in (*10*). Key results from the analysis are as follows. The separation distribution does not appear to change much at different points along the approach path. The left tail of separation (corresponding to the smallest separation values) does not appear to be heavy-tailed. This is positive from a safety perspective. If we extrapolate this behavior beyond the observed data, we conjecture that smaller separations have probabilities that rapidly decay to effectively zero. Estimates of the final-approach separation variability are consistent with previously published results. Lateral positions near the threshold do not appear to be heavy tailed either. Future work will involve integrating these distributions into probabilistic models of wake vortex behavior.

ACKNOWLEDGEMENT

This work has been supported by NASA and Northwest Research Associates (NWRA) through sub-agreement #NWRA-08-S-114.

REFERENCES

1. Shortle, J., and B. Jeddi. Using Multilateration Data in Probabilistic Analysis of Wake Vortex Hazards for Landing Aircraft. In *Transportation Research Record: Journal of the Transportation Research Board*, No. 2007, Transportation Research Board of the National Academies, Washington, D.C., 2007, pp. 90-96.
2. Shortle, J. A Comparison of Wake-Vortex Models for Use in Probabilistic Aviation Safety Analysis. In *Proceedings of the International System Safety Conference*, A. G. Boyer, N. J. Gauthier (eds.), Baltimore, MD, 2007, pp. 581-589.
3. Boswell, S. Evaluation of the Capacity and Delay Benefits of Terminal Air Traffic Control Automation. DOT/FAA/RD-92/28, MIT Lincoln Laboratory, 1993.
4. Haynie, C. An Investigation of Capacity and Safety in Near-terminal Airspace Guiding Information Technology Adoption. Ph.D. Dissertation, George Mason University, 2002.
5. Xie, Y. Quantitative Analysis of Airport Arrival Capacity and Arrival Safety using Stochastic Models. Ph.D. Dissertation, George Mason University, 2005.
6. Ballin, M., and H. Erzberger. An Analysis of Landing Rates and Separations at the Dallas / Fort Worth International Airport. NASA Technical Memorandum 110397, 1996.
7. Andrews, J., and J. Robinson. Radar-Based Analysis of the Efficiency of Runway Use. AIAA Guidance, Navigation & Control Conference, Montreal, Quebec. AIAA-2001-4359, 2001.
8. Rakas, J., and H. Yin. Statistical Modeling and Analysis of Landing Time Intervals: Case Study of Los Angeles International Airport, California. In *Transportation Research Record: Journal of the Transportation Research Board*, No. 1915, Transportation Research Board of the National Academies, Washington, D.C., 2005, pp. 69-78.
9. Levy, B., J. Legge, and M. Romano. Opportunities for Improvements in Simple Models for Estimating Runway Capacity, 23rd Digital Avionics Systems Conference, Salt Lake City, UT, 2004.

10. Jeddi, B., J. Shortle, and L. Sherry. Statistics of the Approach Process at Detroit Metropolitan Wayne County Airport. In *Proceedings of the International Conference on Research in Air Transportation*, Belgrade, Serbia and Montenegro, 2006, pp. 85-92.
11. Jeddi, B., G. Donohue, and J. Shortle. A Statistical Analysis of the Aircraft Landing Process. *Journal of Industrial and Systems Engineering*, Vol. 3, No. 3, 2009, pp. 152-169.
12. Hall, T., and M. Soares. Analysis of Localizer and Glide Slope Flight Technical Error. 27th Digital Avionics Systems Conference. St. Paul, MN, 2008.
13. Harrison, D. Some Preliminary Results of Estimating the Probability of Vertical Overlap from the Distribution of Single Aircraft Deviations from North Atlantic Traffic. UK CAA report, 1987.
14. Campos, L., and J. Marques. On Safety Metrics Related to Aircraft Separation. *Journal of the Royal Naval Society*, Vol. 55, 2002, pp. 39-63.
15. Campos, L., and J. Marques. On a Combination of Gamma and Generalized Error Distributions with Applications to Flight Path Deviations. *Communications in Statistics: Theory and Methods*, Vol. 33, No. 10, 2004, pp. 2307-2332.
16. FAA. 2006. Order 7110.65R. Air Traffic Control.
17. Vandevenne, H., and M. Lippert. Using Maximum Likelihood Estimation to Determine Statistical Model Parameters for Landing Time Separations. 92PM-AATT-0006, MIT Lincoln Laboratory, 2000.
18. Lebron, J. Estimates of Potential Increases in Airport Capacity Through ATC System Improvements in the Airport and Terminal Areas. FAA-DL5-87-1, 1987.
19. Jeddi, B., J. Shortle, and L. Sherry. Statistical Separation Standards for the Aircraft-Approach Process, *Proceedings of the 25th Digital Avionics Systems Conference*, Portland, OR, 2A1-1 – 2A1-13, 2006.

Figure Titles

FIGURE 1: Diagram of DTW airport
FIGURE 2: Boxed region of multilateration data
FIGURE 3: Corrected altitude measurements
FIGURE 4: Comparison of ASPM and multilateration arrival counts
FIGURE 5: Time separation distribution (22R)
FIGURE 6: Time separation at various distances from threshold (22R)
FIGURE 7: Lateral position of aircraft (21L)
FIGURE 8: Left-tail of separation time (22R)
FIGURE 9: Left and right tail of lateral position (1 nm from threshold, 21L)

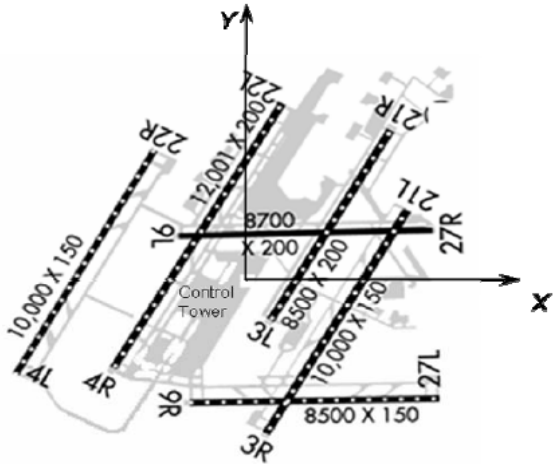

FIGURE 1: Diagram of DTW airport

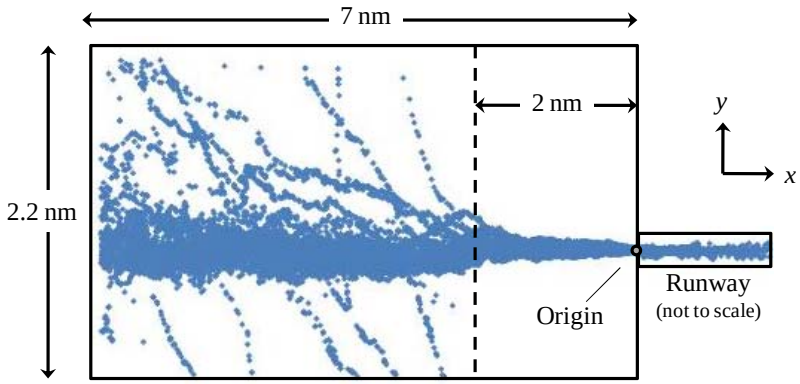

FIGURE 2: Boxed region of multilateration data

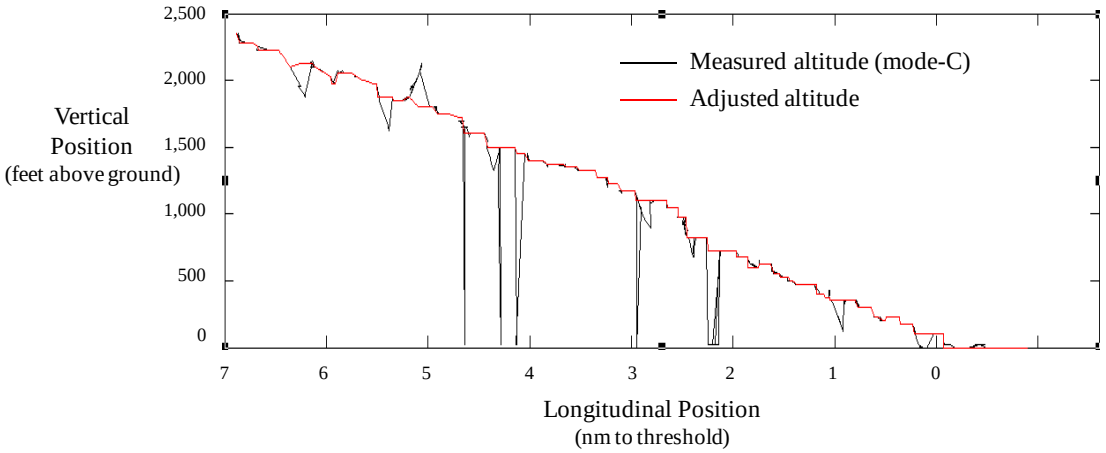

FIGURE 3: Corrected altitude measurements

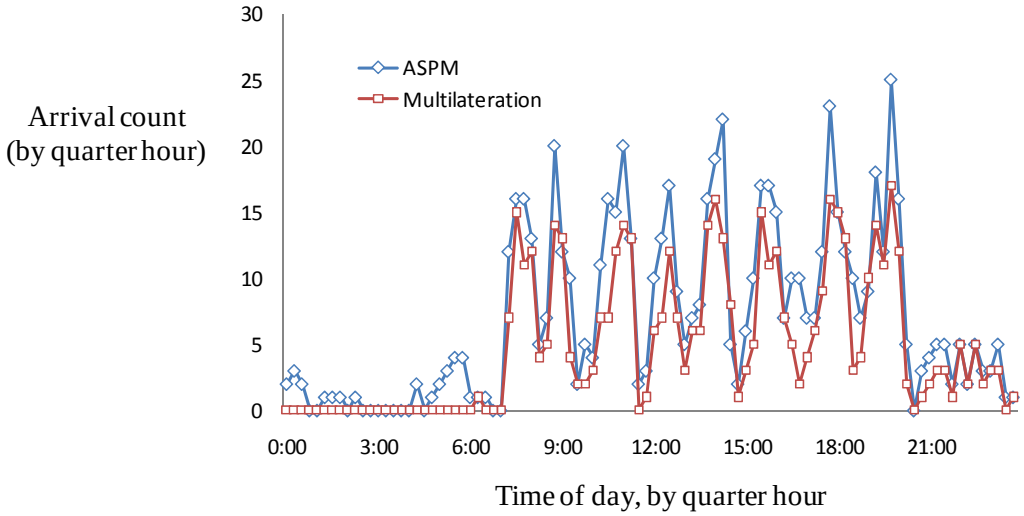

FIGURE 4: Comparison of ASPM and multilateration arrival counts

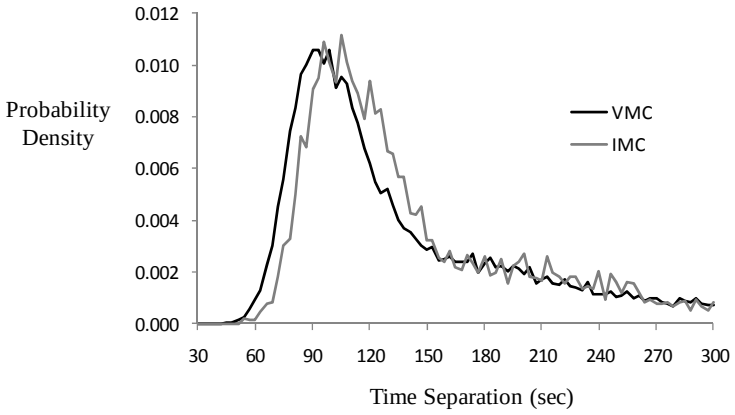

FIGURE 5: Time separation distribution (22R)

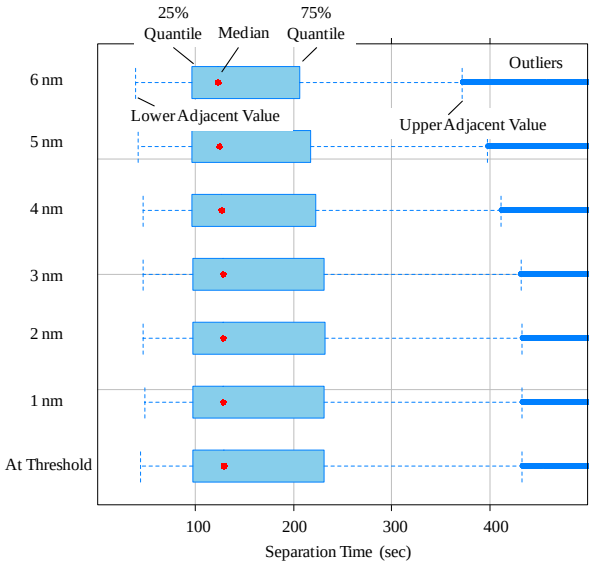

FIGURE 6: Time separation at various distances from threshold (22R)

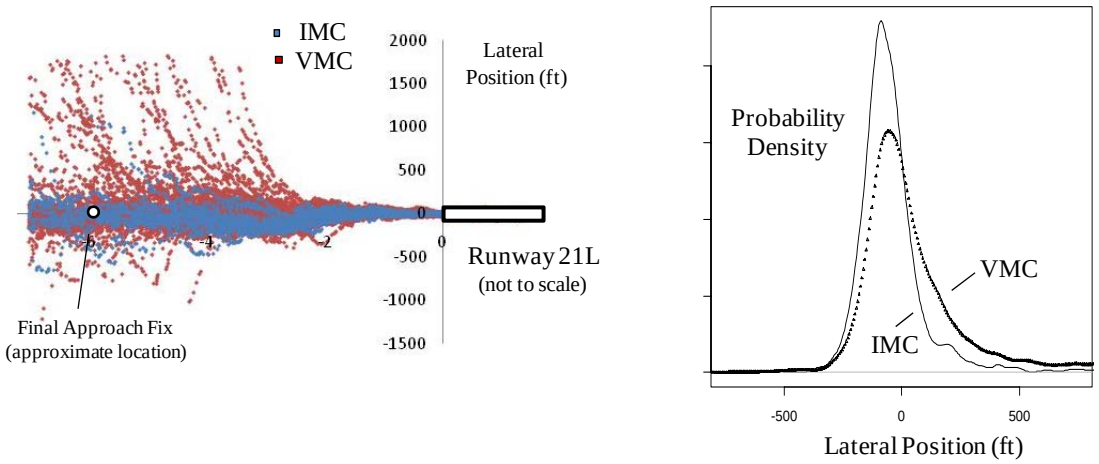

FIGURE 7: Lateral position of aircraft (21L)

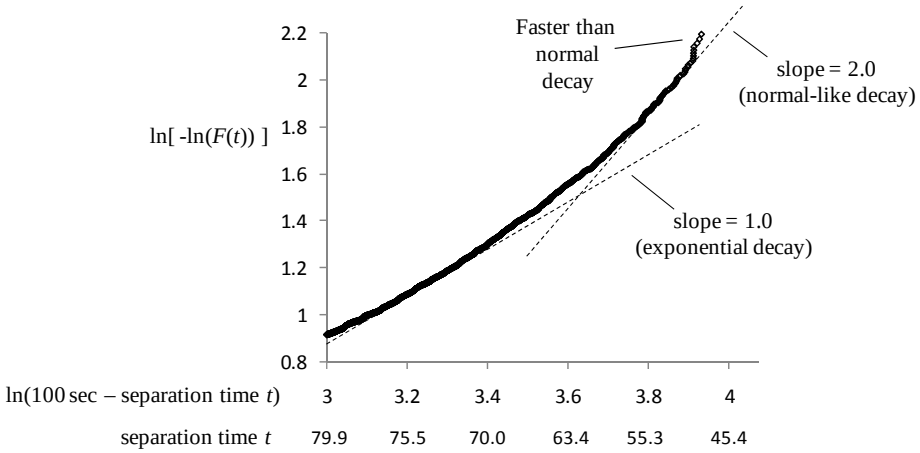

FIGURE 8: Left-tail of separation time (22R)

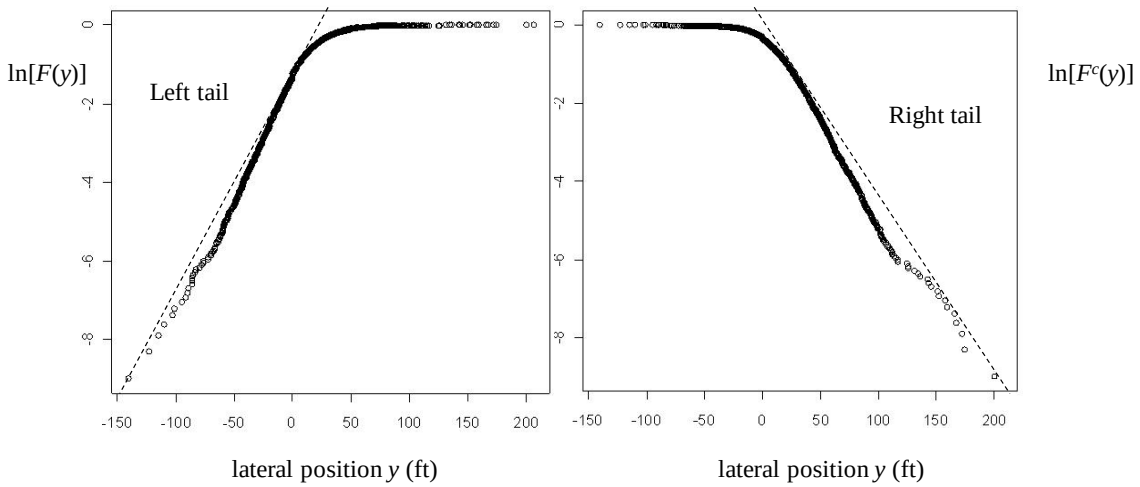

FIGURE 9: Left and right tail of lateral position (1 nm from threshold, 21L)